Journal of Thermal Analysis and Calorimetry, Vol. 95 (2009) 2, 483–487

EFFECT OF ATMOSPHERIC WATER VAPOR ON THE KINETICS OF THERMAL DECOMPOSITION OF COPPER(II) CARBONATE HYDROXIDE

N. Koga, T. Tatsuoka and Y. Tanaka*

Chemistry Laboratory, Graduate School of Education, Hiroshima University, 1-1-1 Kagamiyama Higashi-Hiroshima 739-8524, Japan

The effect of atmospheric water vapor on the kinetic rate behavior of the thermal decomposition of copper(II) carbonate hydroxide, $Cu_2CO_3(OH)_2$, was investigated by means of TG-DTA coupled with a programmable humidity controller. With increasing water vapor pressure $p(H_2O)$ from 0.8 to 10.6 kPa, a systematic reduction of the reaction temperature of the thermal decomposition was observed as the continuous trend from the previous works at the lower $p(H_2O)$. Through a comparative kinetic analysis of the reaction at different $p(H_2O)$, a catalytic action of the atmospheric water vapor on the nucleation process at the first half of the reaction was identified as the possible origin of the reduction of the reaction temperature.

Keywords: *copper(II) carbonate hydroxide, kinetics, malachite, thermal decomposition, water vapor*

Introduction

Copper(II) carbonate hydroxide (CCH) $Cu_2CO_3(OH)_2$, corresponding to the mineral malachite, is one of the precursors for synthesizing CuO through thermal decomposition route. Due to relatively lower reaction temperature of the thermal decomposition, growth of the crystalline particles of CuO is limited during the thermal decomposition processes. As the result, finely dispersed and/or nano-sized CuO particles with higher reactivity are obtained as the solid product [1]. The thermal decomposition of CCH, characterized by a single mass-loss step which evolves CO_2 and H_2O simultaneously, has long been subjected to the kinetic studies by means of various thermoanalytical techniques [2–10]. Our recent interest on this rather well-clarified kinetic process is concerning the feedback effects of the self-generated CO_2 and H_2O on the kinetic rate behavior of the thermal decomposition. We have found [11] that the reaction temperature of the thermal decomposition shifts to the lower temperature region by the effect of self-generated gases. The abnormal behavior from the viewpoint of chemical equilibrium has been reconfirmed by applying controlled rate thermal analysis (CRTA) [12]. Further, with development of an instrument of controlled rate evolved gas analysis coupled with TG (CREGA-TG) [13], the respective effects of CO_2 and H_2O on the thermal decomposition were characterized as the normal effect in view of chemical equilibrium and catalytic effect in view of reaction kinetics, respectively. Through the previous works, the increasing catalytic effect of atmospheric H_2O has been confirmed in the range of water vapor pressure $p(H_2O)$ from ~10^{-3} to 1.5 kPa.

In the present study, we focused on the catalytic action of the atmospheric water vapor on the thermal decomposition of CCH. By applying TG-DTA coupled with a programmable humidity controller, the rate behavior of the thermal decomposition was investigated in the region of $p(H_2O)$ higher than those in the previous studies. Through systematic kinetic analysis of the reaction processes at various $p(H_2O)$, possible origin of the catalytic action is discussed from the viewpoint of overall kinetics.

Experimental

The same batch of CCH prepared and identified in our previous studies [11–14] was utilized after confirming by powder X-ray diffractometry, FTIR spectroscopy and TG-DTA that there is no degeneration by ageing.

The sample of ca. 10.0 mg was weighed into a platinum cell (5 mm in diameter and 2.5 mm in height). By keeping the sample at 350 K in an instrument of TG-DTA (Rigaku TG-8120), a mixed gas of N_2–H_2O with a controlled $p(H_2O)$ generated in a programmable humidity controller (Rigaku HUM-1) was introduced into the reaction tube at a rate of ca. 400 cm^3 min^{-1}. After stabilizing for 30 min, the sample was heated at various heating rates β for recording TG-DTA curves.

* Author for correspondence: nkoga@hiroshima-u.ac.jp

1388–6150/$20.00

Akadémiai Kiadó, Budapest, Hungary
Springer, Dordrecht, The Netherlands

Results and discussion

Figure 1 shows typical TG-DTG curves for the thermal decomposition of CCH at various $p(H_2O)$ (β=5.0 K min^{-1}). Although the thermal decomposition proceeds in a single mass-loss step, the reaction temperature shifts systematically to the lower temperatures with increasing atmospheric $p(H_2O)$. This is the continuous trend from the lower $p(H_2O)$ region (~10^{-3} Pa) reported previously [11–13]. In Fig. 2, the change of the DTG curves depending on $p(H_2O)$ was reproduced as the changes of the extrapolated onset temperature, $T_{e.o.}$, and peak top temperature, T_p. Accompanying with the increase of $p(H_2O)$ from 0.8 to 10.6 kPa, both $T_{e.o.}$ and T_p decrease more than 30 K, where the most distinguished reduction of the reaction temperature was observed in the $p(H_2O)$ range from 1.2 to 6.8 kPa.

By selecting three different controlled $p(H_2O)$, i.e., 1.2, 4.2 and 6.8 kPa, the kinetic rate data of the thermal decomposition at the respective $p(H_2O)$ were recorded as TG curves at various β from 1.0 to 5.0 K min^{-1}. As the example, the series of TG-DTG curves for the thermal decomposition at $p(H_2O)$= 4.2 kPa is shown in Fig. 3. From the series of kinetic rate data, the apparent activation energies, E_a, at various fractional reaction α were determined by Friedman method [15] according to the following equation.

$$\ln\frac{d\alpha}{dt}=\ln[Af(\alpha)]-\frac{E_a}{RT} \quad (1)$$

where A and $f(\alpha)$ are the pre-exponential factor and kinetic model function, respectively. The Friedman plots of $\ln(d\alpha/dt)$ *vs.* T^{-1} at various α from 0.1 to 0.9 in steps of 0.1 for the kinetic rate data at $p(H_2O)$= 4.2 kPa are shown in Fig. 4. Irrespective of α, the data points at the restricted α form a line and the slopes of the respective Friedman plots at different α are nearly constant. The comparable results of the Friedman plots were obtained also for the kinetic rate data at $p(H_2O)$ of 1.2 and 6.8 kPa, indicating that the isoconversional relationship in Eq. (1) is satisfied by

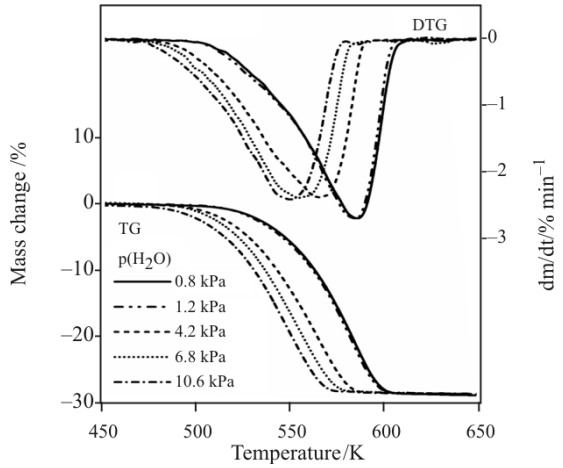

Fig. 1 Influences of $p(H_2O)$ on the TG-DTG curves for the thermal decomposition of CCH at β=5.0 K min^{-1}

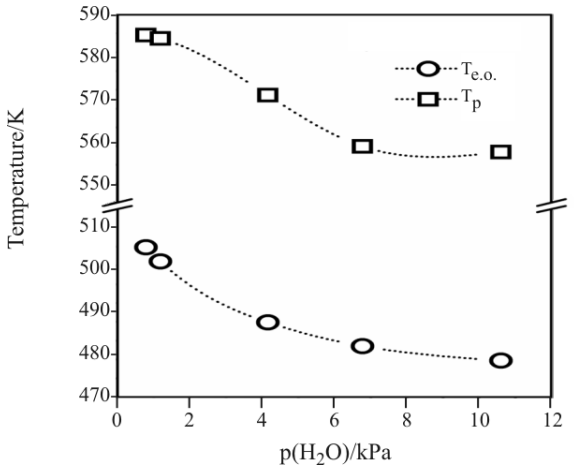

Fig. 2 Influences of $p(H_2O)$ on the $T_{e.o.}$ and T_p of the thermal decomposition of CCH at β=5.0 K min^{-1}

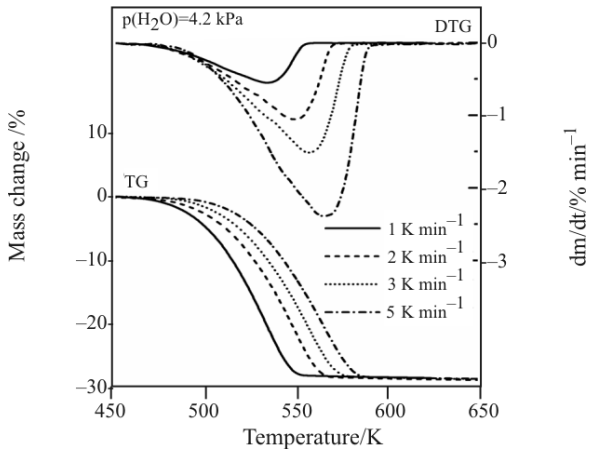

Fig. 3 Influences of β on the TG-DTG curves for the thermal decomposition of CCH at $p(H_2O)$=4.2 kPa

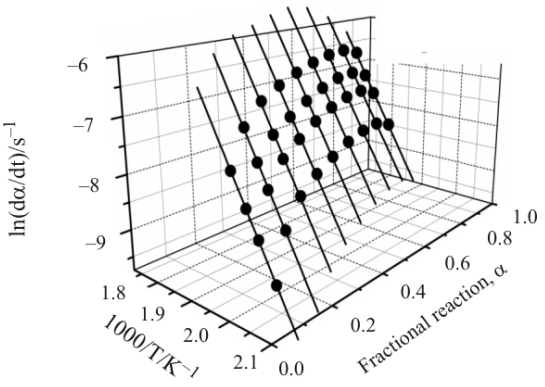

Fig. 4 Typical Friedman plots for the thermal decomposition of CCH at $p(H_2O)$=4.2 kPa

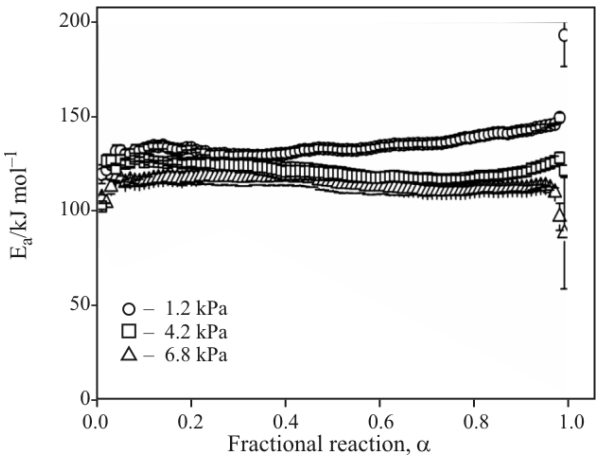

Fig. 5 The α-dependence of E_a for the thermal decomposition of CCH at different $p(H_2O)$

the kinetic rate data of the present reaction at rather high $p(H_2O)$.

Figure 5 compares the values of E_a at various α for the reactions at different $p(H_2O)$. As was expected from the constant slope of the Friedman plots at different α, the values of E_a calculated from the slopes of Friedman plots are nearly constant during the whole course of reaction at the respective $p(H_2O)$. Table 1 lists the values of E_a averaged over $0.1 \le \alpha \le 0.9$. It is worth noting that the values of E_a decrease slightly but systematically with increasing $p(H_2O)$.

For drawing the experimental master plots [16, 17] at a constant temperature for the reactions at different $p(H_2O)$, the kinetic rate data were extrapolated to infinite temperature according to the isoconversional relationship [18, 19].

$$\left(\frac{d\alpha}{d\theta}\right)_\alpha = \left(\frac{d\alpha}{dt}\right)\exp\left(\frac{E_a}{RT}\right)$$

where

$$\theta = \int_0^t \exp\left(-\frac{E_a}{RT}\right)dt \qquad (2)$$

where θ is the generalized time introduced by Ozawa [20–22], indicating the reaction time at infinite temperature. The averaged values of E_a listed in Table 1 were utilized for this procedure. Figure 6 compares the experimental master plots at infinite temperature, i.e., $d\alpha/d\theta$ *vs.* α, for the reactions at different $p(H_2O)$, where apparent change of experimental master plot with $p(H_2O)$ is observed. Although all the experimental master plots are decelerate, the experimental master plot at $p(H_2O)$=1.2 kPa is characteristic indicating two decelerate processes with apparently different slopes. With increasing $p(H_2O)$, the difference of the slopes decreases.

Because the value of $d\alpha/d\theta$ at a selected α corresponds to the exponential value of the intercept of the Friedman plot, the following equation is derived [18, 19].

$$\frac{d\alpha}{d\theta} = Af(\alpha) \qquad (3)$$

For the ideal cases, $f(\alpha)$ derived on the basis of physico-geometric models of reaction mechanisms are utilized for describing the rate process [23]. In the present case characterized by two different decelerate processes, however, the whole course of the reaction can not be described by a single physico-geometric $f(\alpha)$. For the first sake of apparent curve fitting, an empirical kinetic model known as Šesták–Berggren model with three kinetic exponents [24], SB(m, n, p), was employed.

$$f(\alpha) = \alpha^m (1-\alpha)^n [-\ln(1-\alpha)]^p \qquad (4)$$

On the basis of Eq. (3), the best values of the kinetic exponents in SB(m, n, p) and the value of A were determined simultaneously through the nonlinear least square fitting by the Levenberg–Marquardt optimization algorithm [25, 26]. The most appropriate SB(m, n, p) function and the value of A for fitting the experimental master plot in the α range from 0.1 to 0.9 were listed in Table 1, together with the drawings of the fitting curves in Fig. 6. Although it is difficult

Table 1 Kinetic parameters evaluated for the thermal decomposition of CCH at different $p(H_2O)$

$p(H_2O)$/kPa	E_a/kJ mol^{-1}	Range of α	$f(\alpha)$	A/s^{-1}	γ^2
1.2	133.8±3.6	$0.1 \le \alpha \le 0.9$	SB(–4.07, 1.88, 3.63)	$(1.88\pm0.02)\cdot10^9$	0.9999
		$0.1 \le \alpha \le 0.4$	JMA(0.85)	$(4.26\pm0.03)\cdot10^9$	0.9854
		$0.6 \le \alpha \le 0.9$	JMA(2.04)	$(2.46\pm0.06)\cdot10^9$	0.9960
4.2	120.7±3.2	$0.1 \le \alpha \le 0.9$	SB(3.75, –0.94, –3.90)	$(5.10\pm0.15)\cdot10^8$	0.9985
		$0.1 \le \alpha \le 0.45$	JMA(0.89)	$(4.26\pm0.03)\cdot10^8$	0.9989
		$0.65 \le \alpha \le 0.9$	JMA(1.99)	$(2.46\pm0.06)\cdot10^8$	0.9947
6.8	114.6±2.9	$0.1 \le \alpha \le 0.9$	SB(1.33, 0.08, –1.45)	$(1.82\pm0.02)\cdot10^8$	0.9998
		$0.1 \le \alpha \le 0.5$	JMA(0.97)	$(2.28\pm0.01)\cdot10^8$	0.9940
		$0.7 \le \alpha \le 0.9$	JMA(2.18)	$(1.08\pm0.03)\cdot10^8$	0.9987

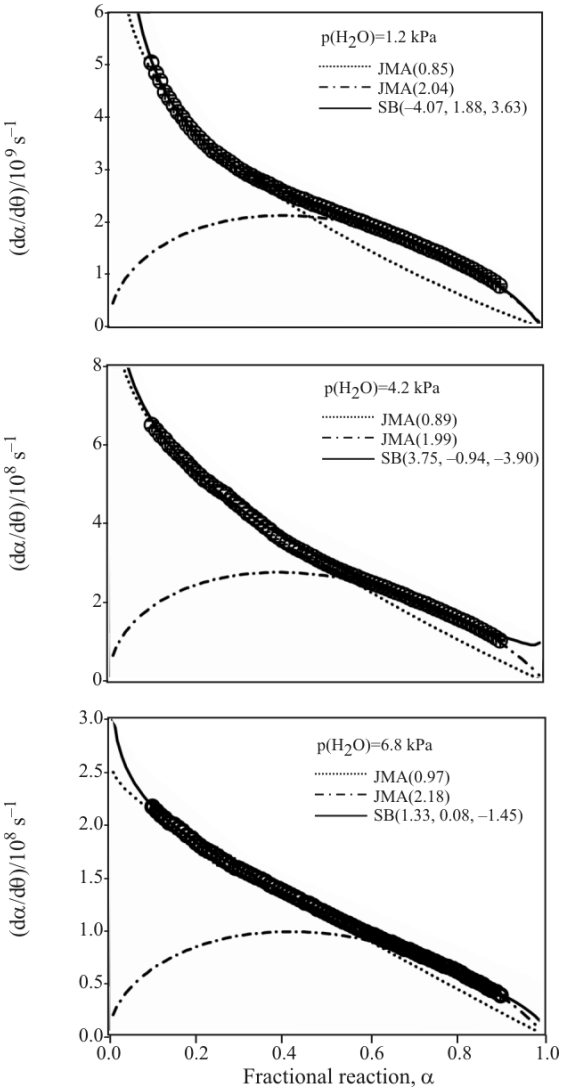

Fig. 6 The experimental master plots of dα/dθ *vs.* α for the thermal decomposition of CCH at different $p(H_2O)$ and the fitting curves drawn by assuming $f(\alpha)$ evaluated by the nonlinear least square fittings

to estimate the physico-geometric significance of the respective kinetic exponents in SB(*m*, *n*, *p*) for the present reaction, the experimental master plots are fitted nearly perfectly by a SB(*m*, *n*, *p*) function due to high flexibility of the empirical model [27] and the $p(H_2O)$-dependent change of the experimental master curve is reflected by the changes of the respective kinetic exponents.

As an alternative approach, the experimental master plots in the α region of the first and second half of the reaction were fitted separately by the physico-geometric $f(\alpha)$ with non-integral kinetic exponent [28–31]. With varying systematically the range of α for fitting, we found that, irrespective of $p(H_2O)$ applied, both the first and second half of the reaction are fitted closely by the nucleation-growth type model JMA(*m*).

$$f(\alpha)=m(1-\alpha)[-\ln(1-\alpha)]^{1-1/m} \quad (5)$$

The best values of kinetic exponent *m* and *A* evaluated by the nonlinear least square fitting in the restricted range of α were listed in Table 1. The respective fitting curves were drawn in Fig. 6. Irrespective of $p(H_2O)$ applied, the kinetic exponents $m\approx1$ and $m\approx2$ were estimated as the best values for the first and second half of the reaction, respectively. By a simple physico-geometric consideration, JMA(*m*) with $m\approx1$ and $m\approx2$ seem to describe the rate processes controlled by the constant rate nucleation and two-dimensional growth of nuclei, respectively. It should be noted here that the α range of the first half reaction which described by JMA(*m*) with $m\approx1$ is extended slightly with increasing $p(H_2O)$, accompanied by the reduction of the α range of the second half reaction described by JMA(*m*) with $m\approx2$. This observation implies that the contribution of the initial reaction stage regulated by the nucleation process increases with $p(H_2O)$. From the view point of the overall kinetics, the reduction of reaction temperature seems to result from the enhancement of the nucleation process by the atmospheric water vapor. Turning the focus on the Arrhenius parameters, the values of *A* for both the first and second half of the reaction decrease with increasing $p(H_2O)$. Accordingly, the reduction of the reaction temperature expected from the decrease in E_a is partially compensated by the interdependent decrease in the value of *A* [32–35].

The catalytic action of the atmospheric water vapor has been reported for many thermal dehydration processes of salt hydrates as the Smith–Topley effect [36–38]. Corresponding to the respective characteristics of the thermal dehydration processes, several mechanistic interpretations for the Smith–Topley effect have been provided [37, 38]. The thermal decomposition of CCH shares several similarities with the thermal dehydration processes which exhibit the Smith–Topley effect, such as the formation of the poorly crystalline solid product under reduced pressure [11], the systematic variation of the kinetic behavior of the surface reaction [11–13], and so on. However, the continuously increasing catalytic action of the atmospheric water vapor in a wide range of $p(H_2O)$ from 10^{-3} to 10.6 kPa were observed for the present decomposition, in contrast to the characteristic behavior of the Smith–Topley effect which indicates a minimum and maximum of the reaction rate in a limited range of $p(H_2O)$ [37, 38]. Further extensive and detailed investigations are apparently required for providing the mechanistic interpretation for the catalytic action of atmospheric water vapor on the thermal decomposition of CCH.

Conclusions

Being continuous with the previous observation at the lower $p(H_2O)$, the reaction temperature of the thermal decomposition of CCH was reduced systematically with the increase of atmospheric $p(H_2O)$ from 0.8 to 10.6 kPa. The value E_a was nearly constant during the course of reaction at a restricted $p(H_2O)$ and decreased with increasing $p(H_2O)$. Within the range of $p(H_2O)$ applied in the present study, the reaction process was characterized by the first and second half of the reaction regulated by the nucleation process and two-dimensional growth, respectively. From the observation of increasing contribution of the nucleation process with $p(H_2O)$, a catalytic action of the atmospheric water vapor on the nucleation process was expected as the possible origin for the reduction of the reaction temperature depending on $p(H_2O)$.

Acknowledgements

The present work was supported partially by a grant-in-aid for scientific research (B) (No. 18300267) from Japan Society for the Promotion of Science.

References

1 N. Koga and H. Tanaka, Kagaku-to-Kyoiku, 54 (2006) 102, in Japanese.
2 P. Ramamurthy and E. A. Secco, Can. J. Chem., 48 (1970) 3510.
3 J. Morgan, J. Thermal Anal., 12 (1977) 245.
4 Z. D. Zivkovic, D. F. Bogosavljevic and V. D. Zlatkovic, Thermochim. Acta, 18 (1977) 235, 310.
5 D. Dollimore and T. J. Taylor, Thermochim. Acta, 40 (1980) 297; Proc. 7th ICTA, Ontario 1982, p. 636.
6 I. W. M. Brown, K. J. D. Mackenzie and G. J. Gainsford, Thermochim. Acta, 74 (1984) 23.
7 I. M. Uznov and D. G. Klissurski, Thermochim. Acta, 81 (1984) 353.
8 H. Tanaka and Y. Yamane, J. Thermal Anal., 38 (1992) 627.
9 M. Reading and D. Dollimore, Thermochim. Acta, 240 (1994) 117.
10 N. Koga, Thermochim. Acta, 258 (1995) 145.
11 N. Koga, J. M. Criado and H. Tanaka, Thermochim. Acta, 340/341 (1999) 387.
12 N. Koga, J. M. Criado and H. Tanaka, J. Therm. Anal. Cal., 60 (2000) 943.
13 N. Koga and S. Yamada, Int. J. Chem. Kinet., 37 (2005) 346.
14 N. Koga and H. Tanaka, J. Therm. Anal. Cal., 82 (2005) 725.
15 H. L. Friedman, J. Polym. Sci. Part C, 6 (1964) 183.
16 F. J. Gotor, J. M. Criado, J. Malek and N. Koga, J. Phys. Chem. A, 104 (2000) 10777.
17 J. M. Criado, L. A. Perez-Maqueda, F. J. Gotor, J. Malek and N. Koga, J. Therm. Anal. Cal., 72 (2003) 901.
18 T. Ozawa, J. Thermal Anal., 31 (1986) 547.
19 N. Koga, Thermochim. Acta, 258 (1995) 145.
20 T. Ozawa, Bull. Chem. Soc. Jpn., 38 (1965) 1881.
21 T. Ozawa, J. Thermal Anal., 2 (1970) 301.
22 T. Ozawa, Thermochim. Acta, 100 (1986) 109.
23 N. Koga and H. Tanaka, Thermochim. Acta, 388 (2002) 41.
24 J. Šesták and G. Berggren, Thermochim. Acta, 3 (1971) 1.
25 D. M. Bates and D. G. Watts, Nonlinear Regression and its Applications, Wiley, New York 1988.
26 N. Koga, A. Mako, T. Kimizu and Y. Tanaka, Thermochim. Acta, 467 (2008) 11.
27 L. A. Perez-Maqueda, J. M. Criado and P. E. Sanchez-Jimenez, J. Phys. Chem. A, 110 (2006) 12456.
28 J. Šesták, J. Thermal Anal., 33 (1988) 1263.
29 R. Ozao and M. Ochiai, J. Ceram. Soc. Jpn., 101 (1993) 263.
30 N. Koga and H. Tanaka, J. Thermal Anal., 41 (1994) 455.
31 N. Koga and J. Malek, Thermochim. Acta, 282/283 (1996) 69.
32 N. Koga, Thermochim. Acta, 244 (1994) 1.
33 A. K. Galwey and M. Mortimer, Int. J. Chem. Kinet., 38 (2006) 464.
34 P. Budrugeac, V. Musat and E. Segal, J. Therm. Anal. Cal., 88 (2007) 699.
35 J. M. Criado, P. E. Sanchez-Jimenez and L. A. Perez-Maqueda, J. Therm. Anal. Cal., 92 (2008) 199.
36 W. E. Garner, Chemistry of Solid-state, Butterworths, London 1955, Chap. 8.
37 M. E. Brown, D. Dollimore and A. K. Galwey, Reactions in the Solid State, Elsevier, Amsterdam 1980, Chap. 4.
38 A. K. Galwey and M. E. Brown, Thermal Decomposition of Ionic Solids, Elsevier, Amsterdam 1999, Chap. 7.

DOI: 10.1007/s10973-008-9271-0